Molecular Pharmacology Fast Forward. Published on October 22, 2018 as DOI: 10.1124/mol.118.112987
This article has not been copyedited and formatted. The final version may differ from this version.

Regulation of a opioid receptor chaperone protein, RTP4, by morphine

Wakako Fujita, Mini Yokote, Ivone Gomes, Achla Gupta, Hiroshi Ueda, and Lakshmi A. Devi

W.F.: Department of Frontier in Life Sciences, Nagasaki University Graduate School of Biomedical Sciences, Nagasaki, 852-8588, Japan

M.Y. and H.U.: Department of Therapeutic Innovation and Pharmacology, Nagasaki University Graduate School of Biomedical Sciences, Nagasaki, 852-8521, Japan

I.G., A.G. and L.A.D.: Department of Pharmacological Sciences, Icahn School of Medicine at Mount Sinai, New York, NY 10029, USA

Molecular Pharmacology Fast Forward. Published on October 22, 2018 as DOI: 10.1124/mol.118.112987
This article has not been copyedited and formatted. The final version may differ from this version.

Running Title: Role of RTP4 in regulation of mu-delta heteromer

b) Corresponding Author:

Wakako Fujita

1-7-1, Sakamoto, Nagasaki, Nagasaki city

Tel: +81 (95) 819-8503

Fax: +81 (95) 819-7736

wakakofu@nagasaki-u.ac.jp

Lakshmi A. Devi

Annenberg Building, Room 19-86

1468 Madison Avenue, New York, NY10029

Tel: 212-241-8345

Fax: 212-996-7214

lakshmi.devi@mssm.edu

c)

Number of Text Pages: 38

Number of Tables: 0

Number of Figures: 6

Number of References: 41

Number of Words in Abstract: 250

Number of Words in Introduction: 600

Number of Words in Discussion: 1516

Molecular Pharmacology Fast Forward. Published on October 22, 2018 as DOI: 10.1124/mol.118.112987
This article has not been copyedited and formatted. The final version may differ from this version.

d) Nonstandard abbreviations

DAMGO	[D-Ala^2, N-Me-Phe^4, Gly^5-ol]-Enkephalin
DOPr	Delta opioid receptor
ELISA	Enzyme linked immunosorbent assay
ER	Endoplasmic reticulum
ERK	Extracellular signal-regulated kinase
GPCR	G protein-coupled receptor
MOPr	Mu opioid receptor
NAcc	Nucleus Accumbens
NTX	Naltrexone
REEP	Receptor expression enhancing protein
RTP4	Receptor transporter protein
RT-qPCR	Reverse transcription quantitative PCR
VTA	Ventral tegmental area

Molecular Pharmacology Fast Forward. Published on October 22, 2018 as DOI: 10.1124/mol.118.112987
This article has not been copyedited and formatted. The final version may differ from this version.

Abstract

Signaling by classic analgesics such as morphine is governed primarily by the relative abundance of opioid receptors at the cell surface and this is regulated by receptor delivery to, and retrieval from, the plasma membrane. While retrieval mechanisms such as receptor endocytosis have been extensively investigated, fewer studies have explored mechanisms of receptor maturation and delivery to the plasma membrane. A previous study implicated receptor chaperone proteins (RTPs) in the latter process. Since not much is known about regulation of RTP expression, we initiated studies examining the effect of chronic morphine administration on the levels of RTPs in the brain. Among the four RTPs, we detect selective and region-specific changes in RTP4 expression; RTP4 mRNA is significantly upregulated in the hypothalamus compared to other brain regions. We examined whether increased RTP4 expression impacted receptor protein levels and find a significant increase in the abundance of Mu opioid receptors (MOPr) but not of other related GPCRS (such as delta opioid, CB_1 cannabinoid or D_2 dopamine receptors) in hypothalamic membranes from animals chronically treated with morphine. Next, we used a cell culture system to show that RTP4 expression is necessary and sufficient for regulating opioid receptor abundance at the cell surface. Interestingly, selective MOPr-mediated increase in RTP4 expression leads to increases in cell surface levels of MOPr-DOPr heteromers and this increase is significantly attenuated by RTP4 siRNA. Together, these results suggest that RTP4 expression is regulated by chronic morphine administration and this, in turn, regulates opioid receptor cell surface levels and function.

Molecular Pharmacology Fast Forward. Published on October 22, 2018 as DOI: 10.1124/mol.118.112987
This article has not been copyedited and formatted. The final version may differ from this version.

Introduction

G protein-coupled receptors (GPCRs) belong to the seven transmembrane receptor family and the majority localize to the cell surface. The levels of GPCRs at the cell surface determine the extent of agonist-induced cellular responses by peptide and other hydrophylic ligands. Activation of these receptors lead to initiation of signaling via diverse signal transduction pathways including G-protein- and beta arrestin-mediated signaling pathways leading to their multiple physiological effects.

While significant effort has been put towards understanding mechanisms regulating receptor endocytosis due to its role in cellular desensitization (see review, Williams et al., 2013), relatively few studies have focused on exploring mechanisms regulating delivery of GPCRs to the plasma membranes. Some of these suggested that chaperone proteins could regulate the glycosylation of GPCRs, an important step for membrane trafficking of receptors (Katada et al., 2004). Other studies have suggested a requirement of chaperone proteins for appropriate targeting to the cell surface membrane (Achour et al., 2008; Williams and Devi, 2010). For example, NinaA for Drosophila rhodopsin; RanBP2 for mammalian cone opsin; ODR-4 for C. elegans chemosensory receptors; RAMPs for the mammalian calcitonin receptor like receptor; receptor expression enhancing proteins (REEPs) and receptor transporter proteins (RTPs) for the mammalian odorant and taste receptors (Saito et al., 2004; Behrens et al., 2006; Achour et al., 2008; Matsunami et al., 2009). In some cases, the chaperone proteins mask the endoplasmic reticulum (ER) retention signal present in GPCRs thereby promoting cell surface receptor expression (Saito et al., 2004). These observations suggest that chaperone proteins play a crucial role in the maturation of GPCRs. However, very little information is available about how the expression or function of these chaperone proteins is regulated. In this study we focused on RTPs and explored a role for their regulation in opioid receptor function.

Molecular Pharmacology Fast Forward. Published on October 22, 2018 as DOI: 10.1124/mol.118.112987
This article has not been copyedited and formatted. The final version may differ from this version.

Opioid receptors, members of Class A GPCRs, bind to and are activated by opiates such as morphine and endogenous opioid peptides such as endorphins, enkephalins and dynorphins. Studies by several groups including ours revealed that mu opioid receptors (MOPr) and delta opioid receptors (DOPr) form heteromers that exhibit pharmacological profiles that are distinct from the individual receptor protomers (Gomes et al., 2000; Rozenfeld and Devi, 2007; Gomes et al., 2011). We have previously reported that RTP4, a member of the receptor transporter protein (RTP) family, plays an important role in the cell surface expression of these receptors. Furthermore, we showed that RTP4 facilitates cell surface expression of the heteromers; co-expression of RTP4 with MOPr and DOPr leads to enhanced cell surface expression as well as decreased ubiquitination of the receptors and that in the absence of RTP4, there is a specific retention of MOPr in the Golgi compartment resulting in decreased cell surface expression of both protomers (Decaillot et al., 2008). These results imply that RTP4 regulates the membrane expression of not only MOPr and DOPr but also of MOPr-DOPr heteromers, thereby playing an important role in influencing the action of exogenous and endogenous opioid ligands. In the context of opioid receptor ligands, we have previously observed that chronic morphine administration can up-regulate the expression of MOPr-DOPr heteromers in brain regions that are important for pain perception, as detected by using a MOPr-DOPr heteromer selective antibody (Gupta et al., 2010). However, the mechanism of up-regulation of MOPr-DOPr heteromers in these brain regions is not clear. More importantly, nothing is known about the mechanisms regulating RTP4 expression in general or by opioid receptor activation in particular. In this study, we examined the effect of morphine administration on RTP4 levels and the contribution of RTP4 to changes in cell surface expression of MOPr-DOPr heteromers *in vitro* and *in vivo*.

Molecular Pharmacology Fast Forward. Published on October 22, 2018 as DOI: 10.1124/mol.118.112987
This article has not been copyedited and formatted. The final version may differ from this version.

Materials and Methods

Cell culture and transfection.

Neuro 2A cells were grown in complete growth medium (E-MEM with 10% FBS and 1% P/S). Cells were transfected with either Flag-MOPr (N2A^{MOPr} cells) or with Flag-MOPr along with RTP4 siRNA (Sigma, St. Louis, MO, USA) using Lipofectamine 2000 according to the manufacturer's protocol (Thermo Fisher Scientific Inc., Waltham, MA, USA). Twenty-four hours after transfection, cells were seeded into 24 well plates, 96 well plates or LabTek chamber for further experiments.

Measurement of Gαi response.

Gαi response was measured by using The CellKey™ System (Molecular Devices, Sunnyvale, CA, USA), based on a label-free technology called Cellular Dielectric Spectroscopy, capable of measuring complex impedance changes in cell monolayers after GPCR activation (an increase in impedance means Gαi activation) as described previously (Zhou et al., 2013). Briefly, naïve or transiently transfected Neuro 2A cells (N2A^{MOPr} cells) (32,000 cells/well) were seeded onto a CellKey^{TM} poly-D-lysine coated 96 well microplate according to their optimum growth conditions on the day prior to the experiment and incubated overnight at 37^{o}C in 5% CO_2. At 30 to 60 min prior to running assay, cells were washed with 150 µL of assay buffer (Hank's Balanced Salt Solution with 20 mM HEPES and 0.1% BSA, pre-warmed at 29^{o}C) followed by addition of 135 µL of the assay buffer. The baseline impedance was measured for 2 min followed by addition of ligands at the final concentration of 1 or 10 µM. The changes in impedance were measured for 20 min after addition of ligands.

Molecular Pharmacology Fast Forward. Published on October 22, 2018 as DOI: 10.1124/mol.118.112987
This article has not been copyedited and formatted. The final version may differ from this version.

Treatment of N2A^{MOPr} cells.

Twenty-four hours after plasmid and/or siRNA transfection, N2A^{MOPr} cells were seeded into a 24 well plate (200,000 cells/ well) in complete growth medium and incubated overnight at 37^{o}C with 5% CO_2. Next day, media was replaced with 500 µL of the complete growth medium containing DAMGO or vehicle at the final concentration of 10 µM and incubated for 24 h at 37^{o}C with 5% CO_2. In one set of experiments, cells were pretreated with naltrexone (NTX) (Sigma) or vehicle at the final concentration of 1 µM for 1 h followed by co-treatment with DAMGO and NTX for 24 h. After ligand treatment, N2A^{MOPr} cells were washed once with cold phosphate buffered saline (PBS) and then collected with 300 µL of cold RLT buffer (QIAGEN, Hilden, Germany). The cell lysates were transferred into an RNase free centrifuge tube and stored at -80°C until they were further processed for RT-qPCR. Stock solutions of DAMGO (Sigma) and NTX were made in water.

RT-qPCR.

RT-qPCR was performed with the above mentioned N2A^{MOPr} cell lysates and with lysates from mouse brain. In the latter case we extracted RNA-containing aqueous solution using the TRIzol reagent according to the manufacturer's protocol (Thermo Fisher Scientific Inc.) before the total RNA purification. Total RNA was purified using RNeasy Mini kit (QIAGEN Inc., Germantown, MD, USA) according to manufacturer's protocol. cDNA was synthesized using the PrimeScript^{TM} RT Master Mix (Takara, Shiga, Japan) according to the manufacturer's protocol. Real-time PCR was performed using the Power SYBR Green qPCR Master Mix (Applied Biosystems, Foster City, CA, USA). The PCR template source was 4 µL of 10-times diluted first-strand cDNA. Amplification was performed with an ABI PRISM 7900HT sequence detection system (Applied Biosystems) or StepOne Real Time PCR system (Applied Biosystems). After an initial denaturation step at 95°C for 10 min, amplification was performed using 45 cycles of denaturation (95°C for 15 s), annealing (55°C for 30 s), and extension (72°C

Molecular Pharmacology Fast Forward. Published on October 22, 2018 as DOI: 10.1124/mol.118.112987
This article has not been copyedited and formatted. The final version may differ from this version.

for 30 s). We amplified GAPDH, a housekeeping gene, as a control. The data were analyzed using the sequence detection system software (version 2.2.1, for ABI PRISM 7900HT Software Applied Biosystems or version 2.3, for StepOne Software, Applied Biosystems) as described in Data Analysis. The software generates the baseline subtracted amplification plot of normalized reporter values (ΔRn) versus cycle number. The amplification threshold was set at 6-7 of the ΔRn linear dynamic range (50-60% of maximum ΔRn). The fractional cycle at which the intersection of amplification threshold and the plot occurs is defined as the threshold cycle (Ct-value) for the plot. Samples that gave a Ct-value within 45 cycles were considered to be positive for the mRNA expression. Then quantitative analysis was performed using the $\Delta\Delta$CT method, as described previously (Margolis et al., 2014).

The forward (F) and reverse (R) primers are as follows:

GAPDH-F	TGAAGGTCGGTGTGAACG
GAPDH-R	CAATCTCCACTTTGCCACTG
RTP1-F	TGGAAGCCCAGTGAGAAGC
RTP1-R	AGCAGAAGTTGCAGCCTGAG
RTP2-F	AGCTTTCTGTTCTTCCTTGGG
RTP2-R	GCCACCTCCATCTTCTCGTAG
RTP3-F	TGCAAGAGGTGAAACCCTGG
RTP3-R	AGGACAGTGGAACCTAGCAAAG
RTP4-F	GGAGCCTGCATTTGGATAAG
RTP4-R	GCAGCATCTGGAACACTGG

Immunocytochemistry.

Molecular Pharmacology Fast Forward. Published on October 22, 2018 as DOI: 10.1124/mol.118.112987
This article has not been copyedited and formatted. The final version may differ from this version.

Twenty-four hours after plasmid and/or siRNA transfection, $N2A^{MOPr}$ cells were seeded into a LabTek chamber (20,000 cells/ well) in complete growth medium and incubated overnight at 37^{o}C with 5% CO_2. Next day, the media was replaced with 250 µL of the complete growth medium containing DAMGO or vehicle at the final concentration of 10 µM and incubated for 24 h at 37^{o}C in 5% CO_2. After ligand treatment, $N2A^{MOPr}$ cells were fixed with methanol/acetone (1:1) solution for 5 min at -30^{o}C and then incubated with blocking buffer containing 3% bovine serum albumin (BSA) in Tris-buffered saline at room temperature for 1 h. The cells were then incubated overnight with primary antibody in blocking buffer at 4^{o}C. Mouse anti-MOPr-DOPr heteromer selective antibody (1:100) (Gupta et al., 2010) or rabbit anti-RTP4 antibody (1:200) (MyBioSource, Inc., San Diego, CA, USA) were used as primary antibodies. After washing with blocking buffer, 3 times each for 5 min, the cells were incubated with secondary antibody in blocking buffer at room temperature for 1 h. Goat anti-mouse IgG (H+L) Cross-Adsorbed, Alexa Fluor 488 (1:500) (Thermo Fisher Scientific Inc.), Goat anti-rabbit IgG (H+L) cross-adsorbed Alexa Fluor 594 (1:500) (Thermo Fisher Scientific Inc.) were used as secondary antibodies. After washing with PBS, 3 times each for 5 min, cells were mounted with prolong diamond antifade mounting media with DAPI (Thermo Fisher Scientific Inc.). The immunofluorescent signal was observed under confocal microscopy (LSM800 with airyscan) (Carl Zeiss Meditec Co., Ltd., Tokyo, Japan). Surface plots were drawn using Image J software. The signal intensity was calculated using Image J software and the co-localized area was calculated using the Zeiss Zen microscope software (ZEN 2.3 SP1, Carl Zeiss Meditec Co., Ltd., Tokyo, Japan). When we determine the signal intensity for the whole cell (Figure 2Ab), we first outline the cells and measure the mean intensity of the area using Image J software. On the other hand, when we analyzed the signal intensity on the area close to the edge of the cell (Figure 2Ac and 2B), the mean signal intensity of randomly selected 10 to 12 points only on the outline of the cell was measured using Image J software.

Molecular Pharmacology Fast Forward. Published on October 22, 2018 as DOI: 10.1124/mol.118.112987
This article has not been copyedited and formatted. The final version may differ from this version.

Animals.

Male C57BL/6 mice (25-35 g; 6-12 wk) were obtained from Jackson Laboratories (Bar Harbor, ME, USA). All mice were maintained on a 12-h light/dark cycle with rodent chow and water available ad libitum, and they were housed in groups of five until testing. Animal studies were carried out according to protocols approved by the Icahn School of Medicine at Mount Sinai Animal Care and Use Committee.

Drug administration.

Morphine sulfate (Sigma) was dissolved in saline. Male C57BL/6 mice were injected with morphine sulfate (10 mg/kg) subcutaneously once a day for 10 days. On the 11th day, mice were euthanized by cervical dislocation and various brain regions were collected and transferred into an RNase free centrifuge tube and stored at -80°C until they were further processed for RT-qPCR.

ELISA.

ELISA was carried out as previously described (Gupta et al., 2010; Fujita et al., 2014). Briefly, mouse brain regions were dissected according to mouse brain atlas (Paxinos and Franklin, 2001) and the membrane fraction (10 µg) was subjected to an ELISA assay using either mouse anti-MOPr-DOPr heteromer selective antibody (1:100), rat anti-MOPr antibody (1:500), rat anti-DOPr antibody (1:500), rat anti-CB1R antibody (1:500) or rabbit anti-D2R antibody (1:500) as primary antibodies. As secondary antibody, anti-mouse IgG (1:1000) (Vector laboratories, Inc., Burlingame, CA, USA), anti-rat IgG (1:1000) (Jackson Immuno Research Laboratories, Inc., West Grove, PA, USA) or anti-rabbit IgG (1:1000) (Vector laboratories) coupled to horseradish peroxidase were used as described previously (Gupta et al., 2007). ELISA for each sample was performed in triplicate.

Molecular Pharmacology Fast Forward. Published on October 22, 2018 as DOI: 10.1124/mol.118.112987
This article has not been copyedited and formatted. The final version may differ from this version.

Data Analysis

The data were expressed as Mean±S.D. Student's *t*-test, one-way ANOVA, two-way ANOVA, one-way MANOVA, two-way MANOVA and multiple-comparison test (Newman–Keuls test, Tukey's test or Bonferroni test) were used to analyze the data. A difference was considered to be significant at $P<0.05$. The GraphPad Software Prism7 and JMP Software 14 were used.

Molecular Pharmacology Fast Forward. Published on October 22, 2018 as DOI: 10.1124/mol.118.112987
This article has not been copyedited and formatted. The final version may differ from this version.

Results

In this study we investigated the effect of chronic morphine administration in mice on the levels of RTP mRNAs in different regions of the brain. In addition, we examined the role of RTP4 in regulation of MOPr-DOPr heteromer formation following MOPr activation *in vivo and in vitro.*

RTP4 is highly expressed in mouse brain.

We first surveyed the gene expression datasets of the mouse brain (based on Affymetrix experiments that can be accessed using BioGPS, http://biogps.org) for relative levels of expression of RTPs. This analysis showed that RTPs (RTP1-4) are differentially expressed in various brain regions and that among the various RTPs, RTP4 exhibited the highest expression (Suppl. Figure 1, upper panel). Next, we quantified the levels of RTP4 in different brain regions by quantitative RT-qPCR. Data from this analysis revealed over 2-fold higher expression of the RTP4 mRNA in midbrain, nucleus accumbens (NAcc), pons, hypothalamus, and ventral tegmental area (VTA) compared to cortex; other brain regions had lower levels (Supplemental Figure 1, lower panel).

RTP4 expression is regulated by chronic morphine administration and this affects receptor abundance of MOPr and MOPr-DOPr heteromer in select brain regions.

Next, we examined whether administration of morphine to mice affected RTP4 mRNA levels in the brain. For this, mice were subjected to repeated morphine administration (10 mg/kg, s.c., once a day for 10 days) following which RTP4 mRNA levels in various brain regions were quantified by RT-qPCR. We detected a significant increase ($P<0.05$) of RTP4 mRNA levels only in the hypothalamus among the different brain regions tested (Figure 1A). There were no significant changes in the mRNA levels of RTP1-3 except for a small decrease in RTP3 mRNA levels in the nucleus accumbens of morphine treated animals (Figure 1B). Next, we examined whether the increases in RTP4 mRNA levels led to an increased in membrane levels of MOPr-

Molecular Pharmacology Fast Forward. Published on October 22, 2018 as DOI: 10.1124/mol.118.112987
This article has not been copyedited and formatted. The final version may differ from this version.

DOPr heteromers in the hypothalamus. For this we carried out ELISA assays with antibodies that selectively recognize receptors in endogenous tissue and compared the abundance of these receptors in hypothalamic membranes from saline -treated animals to the receptors in the hypothalamic membranes of morphine-treated (10 mg/kg, s.c., once a day for 10 days) animals; as controls we used membranes from cortex, nucleus accumbens and VTA. Previous studies characterizing these antibodies used tissues from animals lacking individual receptors to demonstrate the specificity of these antibodies (Gupta et al. 2010). In this study we find that repeated morphine administration leads to a significant increase (P<0.05) in MOPr-DOPr heteromer and MOPr levels but not in DOPr levels or levels of CB1 cannabinoid receptors or D2 dopamine receptors (Figure 1C). This increase is only seen in the hypothalamus but not in the cortex, NAcc, and VTA (Figure 1D).

MOPr activation in N2A^{MOPr} cells causes significant upregulation of RTP4 mRNA levels.

Next, we used Neuro2A cells transfected with MOPr (N2A^{MOPr} cells) as a model system to explore the molecular mechanisms underlying the upregulation of RTP4 mRNA levels in order to dissociate if the RTP4 effects seen *in vivo* are a circuit-based or a cell-based phenomenon. In N2A^{MOPr} cells, we confirmed that DAMGO, the MOPr selective agonist, activates Gαi-mediated signaling using the CellKey™ System, that measures complex impedance changes in cell monolayers after GPCR activation (increase in impedance means Gαi activation) (Figure 2A) and find that this can be blocked by the selective MOPr antagonist, naltrexone (NTX; Figure 3A). A second pulse of DAMGO 24 h after first exposure to the drug gave a significantly reduced (P<0.01) Gαi activation (Figure 2A, 2nd DAMGO), suggesting the development of tolerance to the DAMGO-induced Gαi response.

Molecular Pharmacology Fast Forward. Published on October 22, 2018 as DOI: 10.1124/mol.118.112987
This article has not been copyedited and formatted. The final version may differ from this version.

Next, we examined if like morphine, DAMGO could induce changes in the gene expression of RTP4. For this, we treated N2A^{MOPr} cells with DAMGO for 24 h and found that this led to a significant increase (P<0.05) in RTP4 mRNA levels (Figure 2B). We also examined whether DAMGO treatment modulated the levels of other RTPs (RTP1-3) and found that it significantly increased (P<0.01) the mRNA levels of RTP1 but not of RTP2 or RTP3 (Figure 2B). Interestingly, activation of other class A GPCRs known to be expressed in Neuro2A cells (http://biogps.org) (e.g., dopamine and serotonin receptors) by their respective agonists did not cause significant increases in either RTP4 or the related RTPs (RTP 1- 3; Figure 2B). In addition, we find that DAMGO-mediated increases in RTP4 mRNA levels can be blocked by pre-treating N2A^{MOPr} cells with NTX (Figure 3B). Next, we examined if pre-treatment with the MOPr-DOPr heteromer selective antibody affected DAMGO-mediated increases in RTP4 mRNA levels and find that this pre-treatment had no significant effect on RTP4 mRNA levels (Figure 3C). Since the MOPr-DOPr heteromer selective antibody has been shown to selectively block heteromer-mediated signaling (Gupta et al., 2010), these results suggest that DAMGO-mediated increases in RTP4 mRNA levels occur via MOPr.

MOPr-mediated upregulation of RTP4 mRNA levels leads to increases in MOPr-DOPr abundance.

Next, we examined if DAMGO-mediated increases in RTP4 mRNA levels lead to increases in the abundance of the MOPr-DOPr heteromer. To detect cell surface levels, we carried out immunofluorescence analysis using the MOPr-DOPr heteromer selective antibody in N2A^{MOPr} cells treated without or with DAMGO (10 μM) for 24 h. This analysis revealed that the MOPr-DOPr heteromer exhibits a broad punctate distribution within the cells (Figure 4A). The surface plot analyzed by ImageJ software using the black/white images (Figure 4A) revealed that the signal intensity of the MOPr-DOPr heteromer in DAMGO treated cells was greater than that of control cells (Figure 4B). The quantitative analysis showed a significant increase (P<0.01) in the

Molecular Pharmacology Fast Forward. Published on October 22, 2018 as DOI: 10.1124/mol.118.112987
This article has not been copyedited and formatted. The final version may differ from this version.

signal intensity of MOPr-DOPr heteromer in the entire area of the cell 24 h after treatment with DAMGO (Figure 4C, whole cell). In addition, the signal intensity of MOPr-DOPr heteromer in the selected area close to the edge of the cell was also significantly increased (Figure 4C, edge of the cell). These results indicate that prolonged treatment with DAMGO leads to increased MOPr-DOPr heteromer abundance.

MOPr-mediated increases in MOPr-DOPr heteromer abundance is dependent on RTP4.

Given that DAMGO treatment leads to increases in RTP4 mRNA levels as well as MOPr-DOPr heteromer abundance, we examined if RTP4 is required for heteromer upregulation. For this, we pretreated N2A^{MOPr} cells with RTP4 siRNA prior to DAMGO treatment. We find that this treatment led to no significant increase in the abundance of MOPr-DOPr heteromer in response to DAMGO treament; in contrast, an increase was seen in cells treated with the control siRNA (Figure 5A). We confirmed that RTP4 siRNA treatment led to a significant decrease in the levels of RTP4 mRNA (Figure 5B) and protein (Figures 5C and 5D). These results, showing that a decrease in the expression of RTP4 leads to decreases in MOPr-DOPr levels, indicate that RTP4 plays a role in the maturation of MOPr-DOPr heteromers.

MOPr-mediated upregulation of RTP4 increases co-localization of MOPr-DOPr heteromer with RTP4.

We also examined if treatment of N2A^{MOPr} cells with DAMGO for 24 h increased co-localization between RTP4 and MOPr-DOPr heteromers. For this we co-stained the cells with anti-RTP4 and with MOPr-DOPr heteromer selective antibodies and examined the extent of their co-localization. As expected, in control cells, RTP4 appears to be localized to Golgi- and endoplasmic reticulum (ER)-like intracellular compartments (Figure 6A, upper panel). Interestingly, upon treatment with DAMGO (10 μM for 24 h) we find that RTP4 is detected in the cytosol (Figure 6A, lower panel). Moreover, we find a significant increase the colocalization of

Molecular Pharmacology Fast Forward. Published on October 22, 2018 as DOI: 10.1124/mol.118.112987
This article has not been copyedited and formatted. The final version may differ from this version.

MOPr-DOPr heteromer with RTP4 (i.e., the area of merged yellow signal) upon DAMGO treatment (Figure 6B). These results indicate increased association between RTP4 and MOPr-DOPr heteromers which would support a role for RTP4 in the maturation of this heteromer.

Molecular Pharmacology Fast Forward. Published on October 22, 2018 as DOI: 10.1124/mol.118.112987
This article has not been copyedited and formatted. The final version may differ from this version.

Discussion

In this study we explored a role for RTP family members, previously shown to be involved in targeting odorant and taste receptors to the cell surface (Saito et al, 2004; Behrens et al., 2006), as a chaperone of opioid receptors. Analysis of the gene expression datasets show that these proteins are widely expressed in the brain and periphery (http://biogps.org). Among the different RTPs, RTP4 was previously shown to help target MOPr and DOPr to the cell surface in either HEK-293 or Neuro2A cells (Decaillot et al., 2008). In this study we find that repeated morphine administration leads to brain-region specific modulation of RTP4 mRNA levels, with increased levels being observed in the hypothalamus. Besides RTP4 the only other RTPs that were found to be regulated by repeated morphine treatment were RTP3 whose levels showed a trend of decrease in the NAcc and in the cortex, RTP2 which showed a small trend for increase in the Cortex and VTA, and RTP1 which showed a small trend for increase in the hypothalamus and NAcc. These results suggest a brain-area specific modulation of RTP levels by morphine. Although very little is known about how morphine regulates RTP4 levels one possibility is that repeated administration leads to region-specific adaptations that affect the levels of the transcription factors that bind to the promoter region of RTP4 leading to up-/down-regulation of mRNA levels. Support for this comes from studies showing that chronic morphine treatment leads to differential activation of transcriptions factors in different areas of the brain and this may be dependent on the schedule and dose of morphine administration (reviewed in Ammon-Treiber and Hollt, 2005). Another possibility is that the region-specific adaptations induced by repeated morphine administration affect the stability of the mRNA for RTP4. It is also possible that the adaptations to repeated morphine administration could be brought about by brain region specific modulation of MOPr signaling involving either β-arrestin or mitogen-activated protein kinase signaling instead of the normal Gαi-mediated signaling (Al-Hasani and Bruchas,

2011; Williams et al., 2013). Thus, further studies are needed to elucidate how morphine regulates RTP4 levels in the brain. In addition, with regards to antinociception, it is well known that the hypothalamus regulates the endogenous opioid ligand-mediated descending inhibitory pathway projecting from periaqueductal gray to the nociceptive neurons located in the dorsal horn of spinal cord and thus controls nociceptive input from the periphery (Basbaum and Fields, 1979). It is possible that after chronic morphine administration the endogenous compensatory mechanisms against excessive activation of the opioid system might be occurred in the hypothalamus. Hypothalamus specific knockdown of RTP4 on the development of antinociceptve tolerance to morphine would be needed in the future study.

Although we find that repeated morphine administration modulates RTP4 levels in specific brain regions this does not rule out the modulation of the levels of other chaperone proteins in other brain areas expressing MOPr. This could account for the observation that although levels of RTP4 are decreased in the cortex we observe increases in MOPr, DOPr and MOPr-DOPr heteromers although they are significant only in the case of MOPr. Candidate chaperone proteins for MOPr could include ribophorin I (Ge et al., 2009) that has been shown to target MOPr, or proteins such as DRiP78, ATBP50, RACK1, GEC1, norbin, MRAP or USP4 that have been shown to help in the cell surface targeting of other GPCRs (reviewed in Williams and Devi, 2010). Members of the ubiquitin-specific protease family (USP) would be interesting candidates since USP4 has been shown to function as an Adenosine A2A receptor chaperone helping target it to the cell surface and protect this receptor from ubiquitination and degradation (Milojevic et al., 2006). We previously found that USP8 a member of this family is down-regulated in the quantitative proteomic studies with striatal post-synaptic density fractions of mice treated with escalating doses of morphine for 5 days (Stockton et al., 2015). Thus, further studies are needed to determine the brain-region specific putative MOPr chaperone proteins

Molecular Pharmacology Fast Forward. Published on October 22, 2018 as DOI: 10.1124/mol.118.112987
This article has not been copyedited and formatted. The final version may differ from this version.

that are modulated following chronic treatment with morphine and how the levels of these chaperones are affected under the various paradigms of chronic morphine administration.

Our observations that increased RTP4 mRNA levels led to increases in protein levels of MORr but not DOPr, CB1R and D2R in the hypothalamus would suggest that only certain proteins could function as a chaperone for a given GPCR. This is supported by our data in $N2A^{MOPr}$ cells where we find that activation of dopamine receptors does not lead to significant increases in RTPs mRNA levels. Moreover, studies have shown that RACK1 helps target thromboxane A2 and chemokine CXCR4 receptors to the cell surface but not β2-adrenergic or prostanoid DP receptors (Parent et al., 2008) and GEC1 facilitates the trafficking of KOPr but not MOPr or DOPr to the cell surface (Chen et al., 2006). The robust increases in levels of MOPr protein in the hypothalamus following chronic morphine treatment could be due to an increase in its mRNA levels. However, qRT-PCR analysis did not detect significant changes in MOPr mRNA levels (control=100±36; morphine treated=96±50; data not shown). This would indicate that RTP4 could play a stabilizing effect on MOPr protein level and prevent it from degradation.

In this study we find that repeated morphine administration besides modulating RTP4 mRNA levels, it significantly increases expression of MOPr-DOPr heteromers only in the hypothalamus. This is in contrast to a previous study showing that chronic morphine administration leads to significant increases in MOPr-DOPr heteromers in brain regions involved in pain processing and in the spinal cord (Gupta et al., 2010). These differences could be due to the different paradigms of morphine administration, or additional mechanisms regulating MOPr-DOPr heteromer levels. Our *in vitro* data indicates that RTP4 plays a role in increased MOPr-DOPr heteromer expression. In addition, the control experiments suggest that the maturation of the MOPr-DOPr heteromer under physiological conditions requires endogenous RTP4. However this does not rule out the possibility that there might be both

Molecular Pharmacology Fast Forward. Published on October 22, 2018 as DOI: 10.1124/mol.118.112987
This article has not been copyedited and formatted. The final version may differ from this version.

RTP4-dependent and RTP4-independent mechanisms in the increased MOPr-DOPr heteromer formation *in vivo*. In addition, the *in vitro* study revealed that the possibility of the involvement of RTP4 in the mechanism of development of tolerance to the DAMGO-induced Gαi response that may relate to the side effects of chronic morphine treatment such as development of analgesic tolerance *in vivo*. Thus, further studies are needed to explore mechanisms regulating MOPr-DOPr heteromer expression in different brain regions. In addition, we find that the protein level of MOPr showed a robust (i.e. > 5-fold) increase while the increase of MOPr-DOPr was around 2-fold and there were no changes in DOPr protein levels in hypothalamus after chronic morphine treatment (Figure 1C). These results suggest the possibility that the increase in MOPr-DOPr heteromer formation would depend on the increase of cell surface MOPr. As it is well known, however, prior works on the effects of chronic morphine treatment on regulation of MOPr abundance are controversial. Some paper suggests an increase of plasma membrane binding of MOPr agonist (Fabian et al., 2002), while others have reported down-regulation of MOPr mRNA levels in the mouse brain (Zhu et al., 2012) or no change in MOPr protein levels (Ujcikova et al., 2017). It is probable that these differences are due to the experimental paradigm or brain regions used, as a recent article suggests that the changes in mRNA levels depend on the MOPr splicing variants and on the brain regions (Xu et al., 2015) used.

Besides serving as a chaperone protein for the transport of GPCRs (Behrens et al., 2006; Gifford et al., 2008; Decaillot et al., 2008), RTP4 has been shown to have other physiological roles. RTP4 is one of the interferon-stimulated genes increased in peripheral blood leukocytes after the pregnancy and, thus could be used as a marker of pregnancy particularly in rodents (Sinedino et al., 2017; Ribeiro et al., 2014; Gifford et al., 2008; Kose et al., 2016). In addition, RTP4 plays an important role as a marker of disease incidence in conditions such as hypertension in type 2 diabetic patients, Q-fever, interferon-induced depression, HER2(+) breast cancer and in virus infection (Radkowski et al., 2016; Mehraj et al., 2013; Hoyo-Becerra

Molecular Pharmacology Fast Forward. Published on October 22, 2018 as DOI: 10.1124/mol.118.112987
This article has not been copyedited and formatted. The final version may differ from this version.

et al., 2015; Laurin et al., 2013; Davenport et al., 2015). Studies also indicate that in addition to having antiviral activity, RTP4 is involved in microbiota regulation, and in inflammatory cytokine secretion (Schoggins et al., 2011; Brodziak et al., 2013; Ueta et al., 2011). It is not clear if RTP4 functions as a chaperone under these various scenarios. All these roles underscore the necessity to understand how RTP4 levels are regulated under different conditions and suggest that it could be a target for the development of therapeutics for disease conditions where the levels of this protein are altered.

In conclusion, in this study we find that prolonged MOPr activation leads to increases in RTP4 mRNA levels in mouse brain and N2A^{MOPr} cells. Moreover, we find that in N2A^{MOPr} cells RTP4 is necessary and sufficient to increase cells surface expression of MOPr-DOPr heteromers. This suggests that RTP4 could be a putative therapeutic target for treatment of pain or side effects involving MOPr and/or MOPr-DOPr heteromers.

Acknowledgements

We would like to thank Nikita Trimbake for help with the qRT-PCR assay.

Molecular Pharmacology Fast Forward. Published on October 22, 2018 as DOI: 10.1124/mol.118.112987
This article has not been copyedited and formatted. The final version may differ from this version.

10. Authorship Contributions

Participated in research design: Fujita, Devi

Conducted experiments: Fujita, Gupta, Yokote

Performed data analysis: Fujita, Gomes, Yokote

Wrote or contribute to the writing of the manuscript: Fujita, Ueda, Gomes, Devi

Molecular Pharmacology Fast Forward. Published on October 22, 2018 as DOI: 10.1124/mol.118.112987
This article has not been copyedited and formatted. The final version may differ from this version.

References

Achour L, Labbe-Jullie C, Scott MG and Marullo S (2008) An escort for GPCRs: implications for regulation of receptor density at the cell surface. *Trends Pharmacol Sci* **29**(10): 528-535.

Al-Hasani R and Bruchas MR (2011) Molecular mechanisms of opioid receptor-dependent signaling and behavior. *Anesthesiology* **115**(6): 1363-1381.

Ammon-Treiber S and Hollt V (2005) Morphine-induced changes of gene expression in the brain. *Addict Biol* **10**(1): 81-89.

Basbaum AI and Fields HL (1979) The origin of descending pathways in the dorsolateral funiculus of the spinal cord of the cat and rat: further studies on the anatomy of pain modulation. *J Comp Neurol* **187**(3): 513-531.

Behrens M, Bartelt J, Reichling C, Winnig M, Kuhn C and Meyerhof W (2006) Members of RTP and REEP gene families influence functional bitter taste receptor expression. *J Biol Chem* **281**(29): 20650-20659.

Brodziak F, Meharg C, Blaut M and Loh G (2013) Differences in mucosal gene expression in the colon of two inbred mouse strains after colonization with commensal gut bacteria. *PLoS One* **8**(8): e72317.

Chen C, Li JG, Chen Y, Huang P, Wang Y and Liu-Chen LY (2006) GEC1 interacts with the kappa opioid receptor and enhances expression of the receptor. *J Biol Chem* **281**(12): 7983-7993.

Davenport EE, Antrobus RD, Lillie PJ, Gilbert S and Knight JC (2015) Transcriptomic profiling facilitates classification of response to influenza challenge. *J Mol Med (Berl)* **93**(1): 105-114.

Decaillot FM, Rozenfeld R, Gupta A and Devi LA (2008) Cell surface targeting of mu-delta opioid receptor heterodimers by RTP4. *Proc Natl Acad Sci U S A* **105**(41): 16045-16050.

Fabian G, Bozo B, Szikszay M, Horvath G, Coscia CJ and Szucs M (2002) Chronic morphine-induced changes in mu-opioid receptors and G proteins of different subcellular loci in rat brain. *J Pharmacol Exp Ther* **302**(2): 774-780.

Fujita W, Gomes I, Dove LS, Prohaska D, McIntyre G and Devi LA (2014) Molecular characterization of eluxadoline as a potential ligand targeting mu-delta opioid receptor heteromers. *Biochem Pharmacol* **92**(3): 448-456.

Ge X, Loh HH and Law PY (2009) mu-Opioid receptor cell surface expression is regulated by its direct interaction with Ribophorin I. *Mol Pharmacol* **75**(6): 1307-1316.

Gifford CA, Assiri AM, Satterfield MC, Spencer TE and Ott TL (2008) Receptor transporter protein 4 (RTP4) in endometrium, ovary, and peripheral blood leukocytes of pregnant and cyclic ewes. *Biol Reprod* **79**(3): 518-524.

Gomes I, Ijzerman AP, Ye K, Maillet EL and Devi LA (2011) G protein-coupled receptor heteromerization: a role in allosteric modulation of ligand binding. *Mol Pharmacol* **79**(6): 1044-1052.

Gomes I, Jordan BA, Gupta A, Trapaidze N, Nagy V and Devi LA (2000) Heterodimerization of mu and delta opioid receptors: A role in opiate synergy. *J Neurosci* **20**(22): RC110.

Gupta A, Decaillot FM, Gomes I, Tkalych O, Heimann AS, Ferro ES and Devi LA (2007) Conformation state-sensitive antibodies to G-protein-coupled receptors. *J Biol Chem* **282**(8): 5116-5124.

Gupta A, Mulder J, Gomes I, Rozenfeld R, Bushlin I, Ong E, Lim M, Maillet E, Junek M, Cahill CM, Harkany T and Devi LA (2010) Increased abundance of opioid receptor heteromers after chronic morphine administration. *Sci Signal* **3**(131): ra54.

Hoyo-Becerra C, Liu Z, Yao J, Kaltwasser B, Gerken G, Hermann DM and Schlaak JF (2015) Rapid Regulation of Depression-Associated Genes in a New Mouse Model Mimicking

Interferon-alpha-Related Depression in Hepatitis C Virus Infection. *Mol Neurobiol* **52**(1): 318-329.

Katada S, Tanaka M and Touhara K (2004) Structural determinants for membrane trafficking and G protein selectivity of a mouse olfactory receptor. *J Neurochem* **90**(6): 1453-1463.

Kose M, Kaya MS, Aydilek N, Kucukaslan I, Bayril T, Bademkiran S, Kiyma Z, Ozyurtlu N, Kayis SA, Guzeloglu A and Atli MO (2016) Expression profile of interferon tau-stimulated genes in ovine peripheral blood leukocytes during embryonic death. *Theriogenology* **85**(6): 1161-1166.

Laurin M, Huber J, Pelletier A, Houalla T, Park M, Fukui Y, Haibe-Kains B, Muller WJ and Cote JF (2013) Rac-specific guanine nucleotide exchange factor DOCK1 is a critical regulator of HER2-mediated breast cancer metastasis. *Proc Natl Acad Sci U S A* **110**(18): 7434-7439.

Margolis EB, Hjelmstad GO, Fujita W and Fields HL (2014) Direct bidirectional mu-opioid control of midbrain dopamine neurons. *J Neurosci* **34**(44): 14707-14716.

Matsunami H, Mainland JD and Dey S (2009) Trafficking of mammalian chemosensory receptors by receptor-transporting proteins. *Ann N Y Acad Sci* **1170**: 153-156.

Mehraj V, Textoris J, Ben Amara A, Ghigo E, Raoult D, Capo C and Mege JL (2013) Monocyte responses in the context of Q fever: from a static polarized model to a kinetic model of activation. *J Infect Dis* **208**(6): 942-951.

Milojevic T, Reiterer V, Stefan E, Korkhov VM, Dorostkar MM, Ducza E, Ogris E, Boehm S, Freissmuth M and Nanoff C (2006) The ubiquitin-specific protease Usp4 regulates the cell surface level of the A2A receptor. *Mol Pharmacol* **69**(4): 1083-1094.

Parent A, Laroche G, Hamelin E and Parent JL (2008) RACK1 regulates the cell surface expression of the G protein-coupled receptor for thromboxane A(2). *Traffic* **9**(3): 394-407.

Paxinos G and Franklin KBJ (2001) The Mouse Brain in Stereotaxic Coordinates, 2nd ed. Academic Press.

Radkowski P, Wator G, Skupien J, Bogdali A and Wolkow P (2016) Analysis of gene expression to predict dynamics of future hypertension incidence in type 2 diabetic patients. *BMC Proc* **10**(Suppl 7): 113-117.

Ribeiro ES, Bruno RG, Farias AM, Hernandez-Rivera JA, Gomes GC, Surjus R, Becker LF, Birt A, Ott TL, Branen JR, Sasser RG, Keisler DH, Thatcher WW, Bilby TR and Santos JE (2014) Low doses of bovine somatotropin enhance conceptus development and fertility in lactating dairy cows. *Biol Reprod* **90**(1): 10.

Rozenfeld R and Devi LA (2007) Receptor heterodimerization leads to a switch in signaling: beta-arrestin2-mediated ERK activation by mu-delta opioid receptor heterodimers. *FASEB J* **21**(10): 2455-2465.

Saito H, Kubota M, Roberts RW, Chi Q and Matsunami H (2004) RTP family members induce functional expression of mammalian odorant receptors. *Cell* **119**(5): 679-691.

Schoggins JW, Wilson SJ, Panis M, Murphy MY, Jones CT, Bieniasz P and Rice CM (2011) A diverse range of gene products are effectors of the type I interferon antiviral response. *Nature* **472**(7344): 481-485.

Sinedino LD, Honda PM, Souza LR, Lock AL, Boland MP, Staples CR, Thatcher WW and Santos JE (2017) Effects of supplementation with docosahexaenoic acid on reproduction of dairy cows. *Reproduction* **153**(5): 707-723.

Stockton SD, Jr., Gomes I, Liu T, Moraje C, Hipolito L, Jones MR, Ma'ayan A, Moron JA, Li H and Devi LA (2015) Morphine Regulated Synaptic Networks Revealed by Integrated Proteomics and Network Analysis. *Mol Cell Proteomics* **14**(10): 2564-2576.

Ueta M, Kawai T, Yokoi N, Akira S and Kinoshita S (2011) Contribution of IPS-1 to polyI:C-induced cytokine production in conjunctival epithelial cells. *Biochem Biophys Res Commun* **404**(1): 419-423.

Ujcikova H, Hlouskova M, Cechova K, Stolarova K, Roubalova L and Svoboda P (2017) Determination of mu-, delta- and kappa-opioid receptors in forebrain cortex of rats exposed to morphine for 10 days: Comparison with animals after 20 days of morphine withdrawal. *PLoS One* **12**(10): e0186797.

Williams D and Devi LA (2010) Escorts take the lead molecular chaperones as therapeutic targets. *Prog Mol Biol Transl Sci* **91**: 121-149.

Williams JT, Ingram SL, Henderson G, Chavkin C, von Zastrow M, Schulz S, Koch T, Evans CJ and Christie MJ (2013) Regulation of mu-opioid receptors: desensitization, phosphorylation, internalization, and tolerance. *Pharmacol Rev* **65**(1): 223-254.

Xu J, Faskowitz AJ, Rossi GC, Xu M, Lu Z, Pan YX and Pasternak GW (2015) Stabilization of morphine tolerance with long-term dosing: association with selective upregulation of mu-opioid receptor splice variant mRNAs. *Proc Natl Acad Sci U S A* **112**(1): 279-284.

Zhou L, Lovell KM, Frankowski KJ, Slauson SR, Phillips AM, Streicher JM, Stahl E, Schmid CL, Hodder P, Madoux F, Cameron MD, Prisinzano TE, Aube J and Bohn LM (2013) Development of functionally selective, small molecule agonists at kappa opioid receptors. *J Biol Chem* **288**(51): 36703-36716.

Zhu ZP, Badisa RB, Palm DE and Goodman CB (2012) Regulation of rat MOR-1 gene expression after chronic intracerebroventricular administration of morphine. *Mol Med Rep* **5**(2): 513-516.

Molecular Pharmacology Fast Forward. Published on October 22, 2018 as DOI: 10.1124/mol.118.112987
This article has not been copyedited and formatted. The final version may differ from this version.

Footnotes:

This work was supported by the Japan Society for the Promotion of Science KAKENHI [grant number 16K19214 and grant number 18K06894], the Platform for Drug Discovery, Informatics, and Structural Life Science [grant number 16am0101012j0005] from the Japan Agency for medical Research and Development (AMED), and NIH grants DA008863.

Molecular Pharmacology Fast Forward. Published on October 22, 2018 as DOI: 10.1124/mol.118.112987
This article has not been copyedited and formatted. The final version may differ from this version.

Figure Legends

Figure 1. RTP4 expression is regulated by chronic morphine administration and this affects abundance of MOPr and MOPr-DOPr heteromers. (A and B) Male C57BL/6 mice (5-6/group) were administered with saline or morphine (10 mg/kg, s.c.) once a day for 10 days. On the 11th day, brain regions were collected and RT-qPCR was performed. Data were normalized with GAPDH, an internal control. Data are the mean ± S.D. n=5-6. ***P*<0.01, vs. control group (saline), two-way ANOVA and Bonferroni test (A) or two-way MANOVA (B). (C and D) Male C57BL/6 mice (5-6/group) were administered with saline or morphine (10 mg/kg, s.c.) once a day for 10 days. On the 11th day, hypothalamus, cortex, NAcc, and VTA were collected. Membrane protein (10 µg) was subjected to an ELISA assay using receptor-specific antibodies. Data are the mean ± S.D. n=3-6. ***P*<0.01, **P*<0.05, vs. control group (saline), unpaired *t*-test with welch's correction (C) or two-way MANOVA (D).

Figure 2: MOPr activation in N2A^{MOPr} cells causes significant upregulation of RTP4 mRNA levels. (A) N2A^{MOPr} cells (3.2x10^4 cells/well) were treated without or with DAMGO (10 µM) for 20 min (1st DAMGO) and the Gαi response measured using CellKey system. After 24 h cells were given a second treatment with DAMGO (10 µM) (2nd DAMGO) followed by measurement of the Gαi response. Data are the mean ± S.D. n=8-9. ***P*<0.01 vs. control, ##*P*<0.01 vs. 1st DAMGO, Tukey's test. (B) N2A^{MOPr} cells (2x10^4 cells/well) were treated with DAMGO (10 µM), dopamine (10 µg/mL) or serotonin (10 µg/mL) for 24 h. RT-qPCR was performed with specific primers against RTP1, 2, 3, 4 and GAPDH. Data are the mean ± S.D. n=7-45, ***P*<0.01, **P*<0.05, vs. control, one-way MANOVA and Bonferroni test..

Molecular Pharmacology Fast Forward. Published on October 22, 2018 as DOI: 10.1124/mol.118.112987
This article has not been copyedited and formatted. The final version may differ from this version.

Figure 3: Activation of MOPr in N2A^{MOPr} cells upregulate RTP4 mRNA levels. (A) N2A^{MOPr} cells ($3.2x10^4$ cells/well) were treated with DAMGO (1 or 10 μM) with or without pre-treatment with NTX (1 μM) as described in Materials and Methods and the Gαi response measured using the CellKey system. Data are the mean ± S.D. n=3-12. ***P*<0.01 vs. control, ##*P*<0.01 vs. DAMGO alone, Tukey's test. (B) N2A^{MOPr} cells ($2x10^4$ cells/well) were treated without or with DAMGO (10 μM) for 24 h without or without pre-treatment with NTX (1 μM) for 1 h before addition of DAMGO. RT-qPCR was performed with specific primers against RTP4 and GAPDH. Data are the mean ± S.D. n=6-11, **P*<0.05 vs. control, #*P*<0.05 vs. DAMGO alone, Tukey's test. (C) N2A^{MOPr} cells ($2x10^4$ cells/well) were treated with DAMGO (10 μM) for 24 h without or with pretreatment with MOPr-DOPr heteromer selective antibody (1 μg) for 1 h before addition of DAMGO. RT-qPCR was performed with specific primers against RTP4 and GAPDH. Data are the mean ± S.D. n=6-15, **P*<0.05 vs. control, Tukey's test. n.s.= not significant.

Figure 4: MOPr-mediated upregulation of RTP4 mRNA leads to increases in MOPr-DOPr heteromer abundance. (A) N2A^{MOPr} cells were treated without or with DAMGO (10 μM) for 24 h and the presence of MOPr-DOPr heteromers detected by immunofluorescence with MOPr-DOPr heteromer selective antibody as described in Materials and Methods. Images were taken using a CarlZeiss microscope LSM800. (B) The surface plot of the cell in the dotted square in (A) was analyzed by using Image J software. (C) The signal intensity of the MOPr-DOPr heteromer was measured by ImageJ software. n=196 (control), n=341 (DAMGO 10 μM) (whole cell), n=205 (control), n=381 (DAMGO 10 μM) (the area close to the edge of the cell). ***P*<0.01 vs. control, unpaired *t*-test.

Figure 5: MOPr-mediated increases in MOPr-DOPr heteromer abundance is dependent on RTP4 expression. (A) N2A^{MOPr} cells were transfected with either RTP4 siRNA or control

Molecular Pharmacology Fast Forward. Published on October 22, 2018 as DOI: 10.1124/mol.118.112987
This article has not been copyedited and formatted. The final version may differ from this version.

siRNA and then treated with or without DAMGO (10 μM) for 24 h. Expression levels of MOPr-DOPr heteromers in the area close to the edge of the cell was analyzed by immunofluorescence using MOPr-DOPr heteromer selective antibodies. Images were taken using a CarlZeiss microscope LSM800. n=47 (control siRNA), n=20 (RTP4 siRNA), n=47 (control siRNA + 10 μM DAMGO), n=67 (RTP4 siRNA + 10 μM DAMGO), ***P*<0.01 vs. control-control siRNA, #*P*<0.05 vs. DAMGO-control siRNA, Newman-Keuls test. (B to D) RTP4-siRNA expression decreases RTP4 mRNA and protein levels. $N2A^{MOPr}$ cells were transfected with RTP4 siRNA or control siRNA. After 48 h RTP4 mRNA levels (B) were analyzed by RT-qPCR (n=3, ***P*<0.01 vs. control siRNA, unpaired *t*-test) and RTP4 protein expression levels (C and D) by immunofluorescence using a RTP4 selective antibody. (C) Images were taken using a CarlZeiss microscope LSM800. (D) The signal intensity of RTP4 was measured using Image J software. n=144 (control siRNA), n=188 (RTP4 siRNA), ***P*<0.01 vs. control siRNA, unpaired *t*-test.

Figure 6: Increase in co-localization between RTP4 and the MOPr-DOPr heteromer following MOPr activation. $N2A^{MOPr}$ cells were treated without or with DAMGO (10 μM) for 24 h and analyzed by immunofluorescence using the MOPr-DOPr heteromer selective antibody and a RTP4 selective antibody. (A) Images were taken using CarlZeiss microscope LSM800 (63x oil lens, Airyscan). (B) Co-localized area indicated by yellow signal in the merged image was examined using ZEN software (CarlZeiss microscope). Red: RTP4, Green: MOPr-DOPr heteromer, Blue: DAPI, n=23 (control), n=26 (DAMGO), ***P*<0.01 vs. control, unpaired *t*-test.

Molecular Pharmacology Fast Forward. Published on October 22, 2018 as DOI: 10.1124/mol.118.112987
This article has not been copyedited and formatted. The final version may differ from this version.

Figure 1

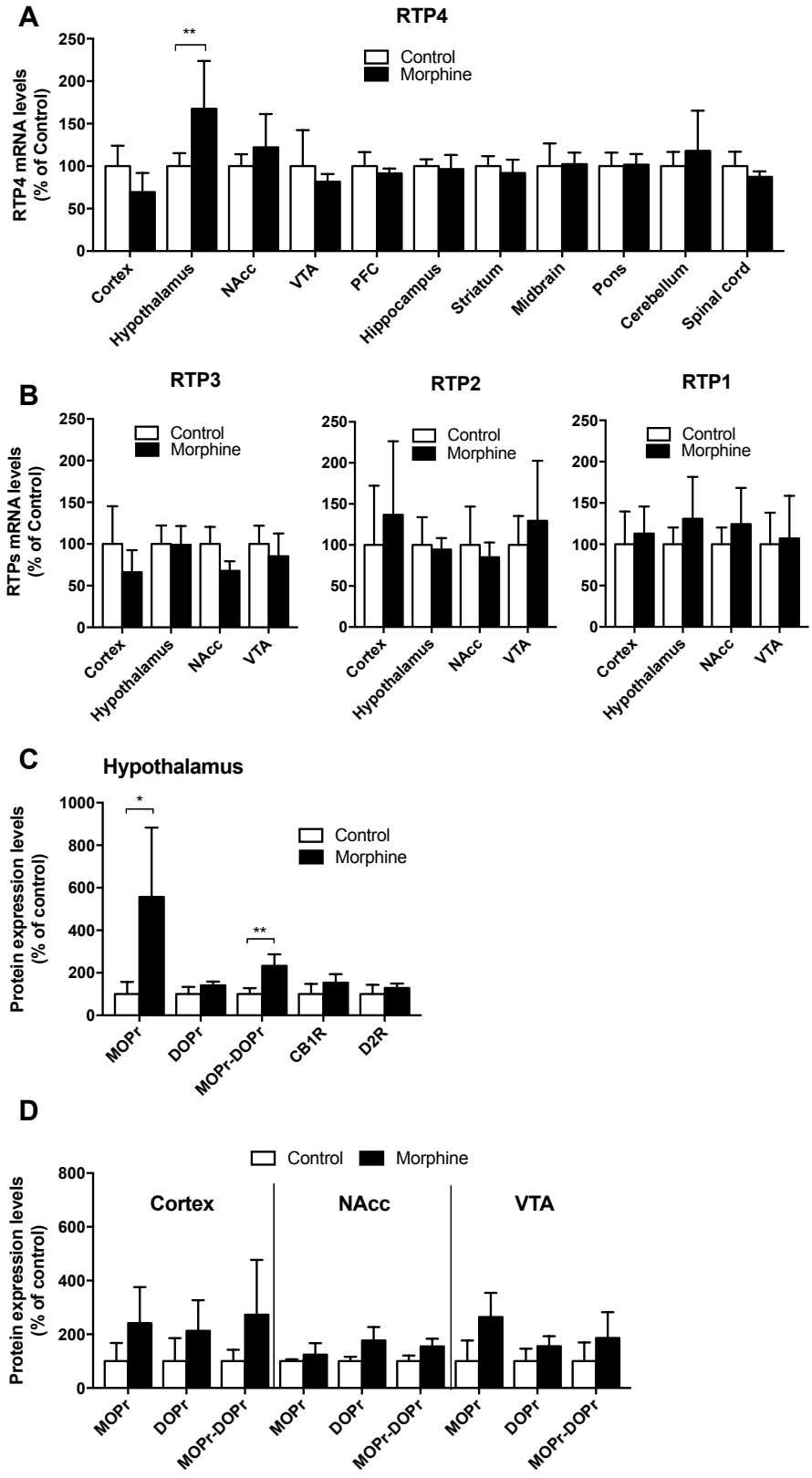

Molecular Pharmacology Fast Forward. Published on October 22, 2018 as DOI: 10.1124/mol.118.112987
This article has not been copyedited and formatted. The final version may differ from this version.

Figure 2

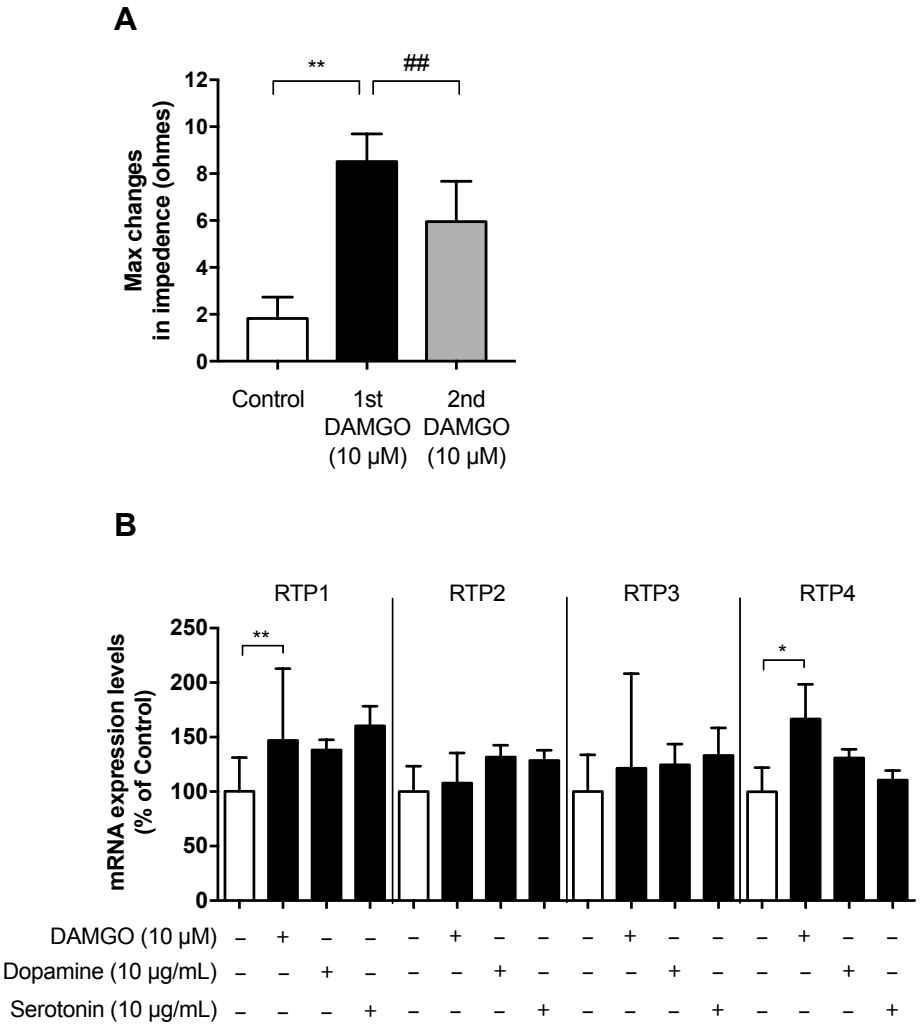

Molecular Pharmacology Fast Forward. Published on October 22, 2018 as DOI: 10.1124/mol.118.112987
This article has not been copyedited and formatted. The final version may differ from this version.

Figure 3

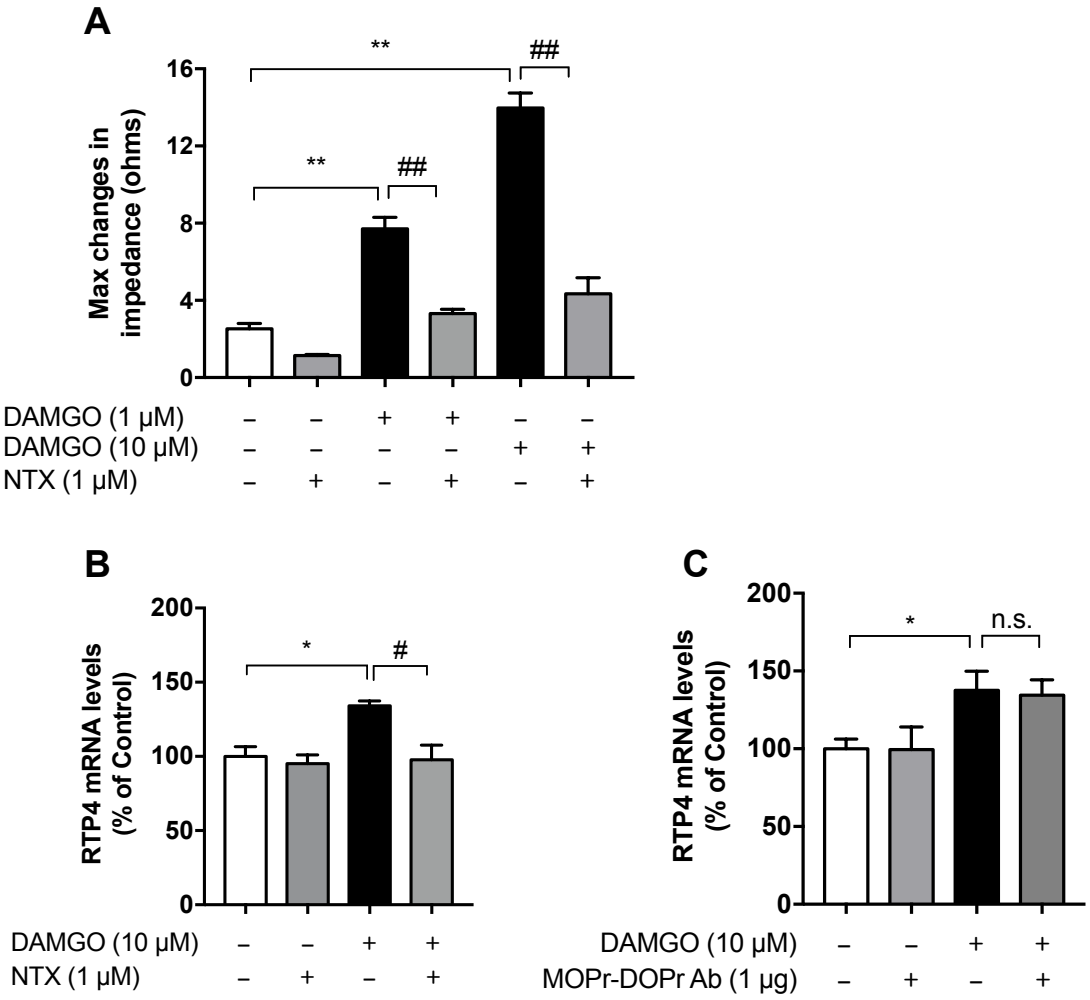

Figure 4

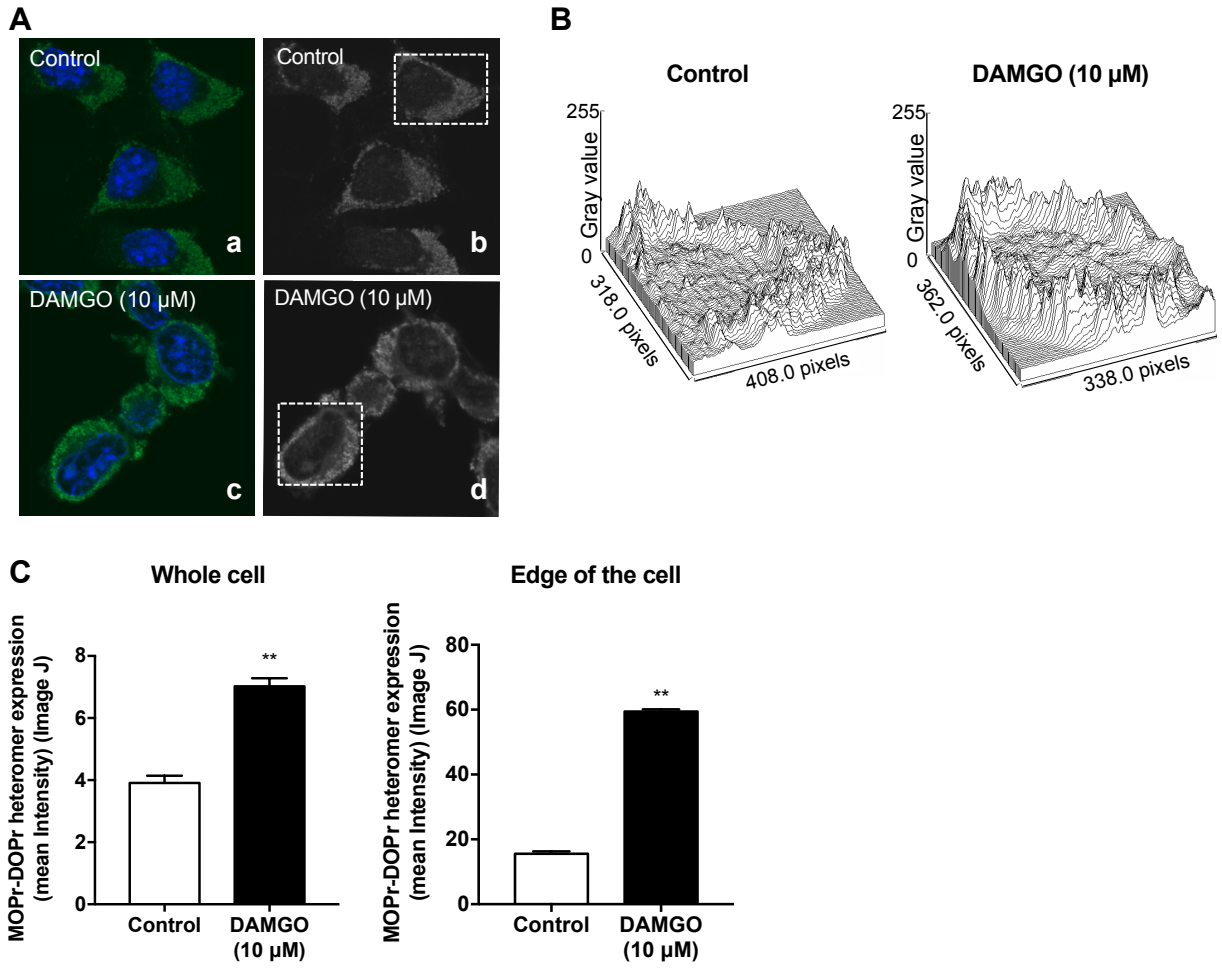
A
Control
a
Control
b
DAMGO (10 μM)
c
DAMGO (10 μM)
d
B
Control
DAMGO (10 μM)
255
Gray value
0
318.0 pixels
408.0 pixels
255
Gray value
0
362.0 pixels
338.0 pixels
C
Whole cell
MOPr-DOPr heteromer expression (mean Intensity) (Image J)
8
6
4
2
0
**
Control
DAMGO (10 μM)
Edge of the cell
MOPr-DOPr heteromer expression (mean Intensity) (Image J)
80
60
40
20
0
**
Control
DAMGO (10 μM)

Figure 5

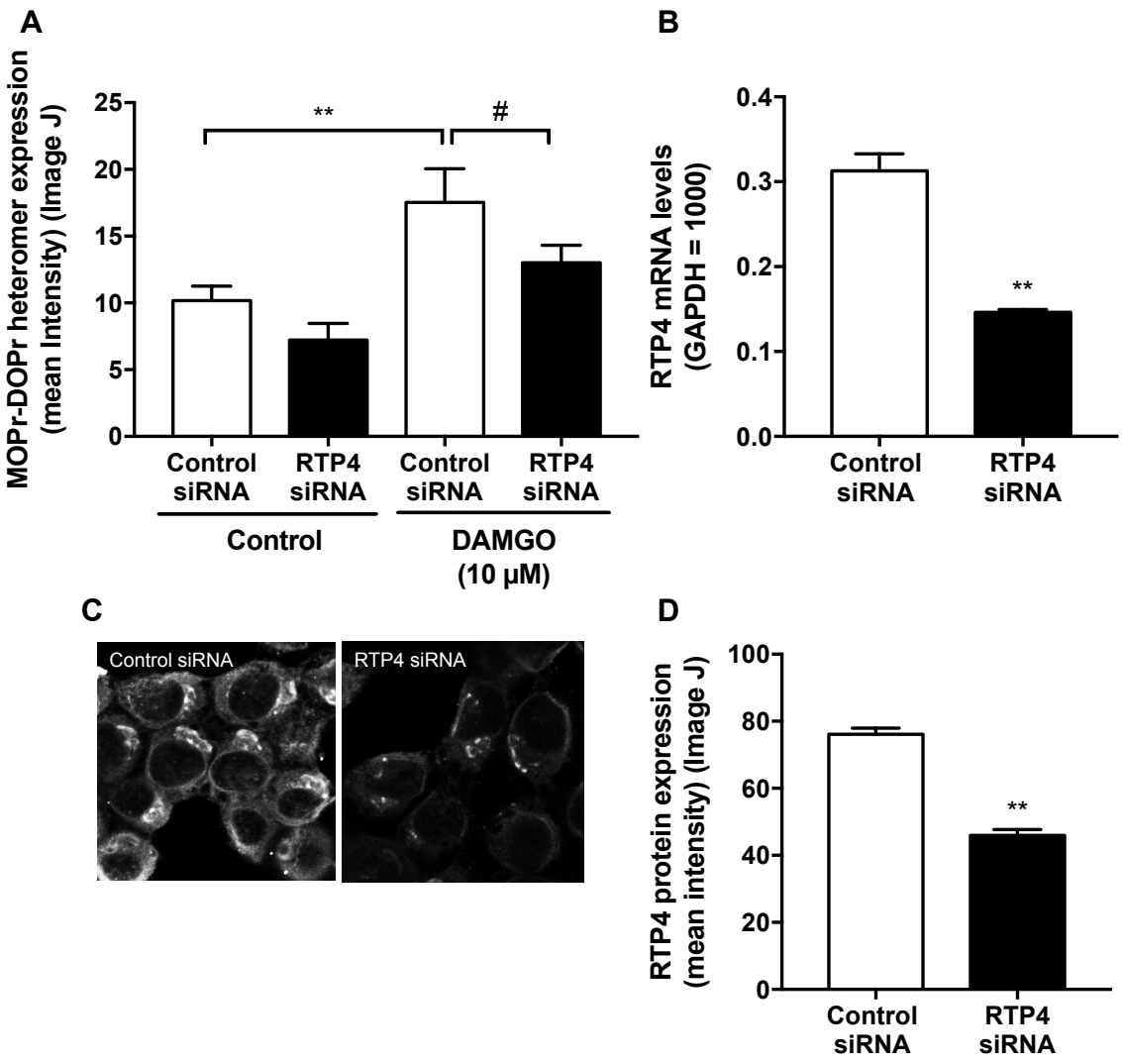
A
MOPr-DOPr heteromer expression (mean Intensity) (Image J)
25
20
15
10
5
0
**
#
Control siRNA
RTP4 siRNA
Control siRNA
RTP4 siRNA
Control
DAMGO (10 μM)
B
RTP4 mRNA levels (GAPDH = 1000)
0.4
0.3
0.2
0.1
0.0
**
Control siRNA
RTP4 siRNA
C
Control siRNA
RTP4 siRNA
D
RTP4 protein expression (mean intensity) (Image J)
100
80
60
40
20
0
**
Control siRNA
RTP4 siRNA

Figure 6

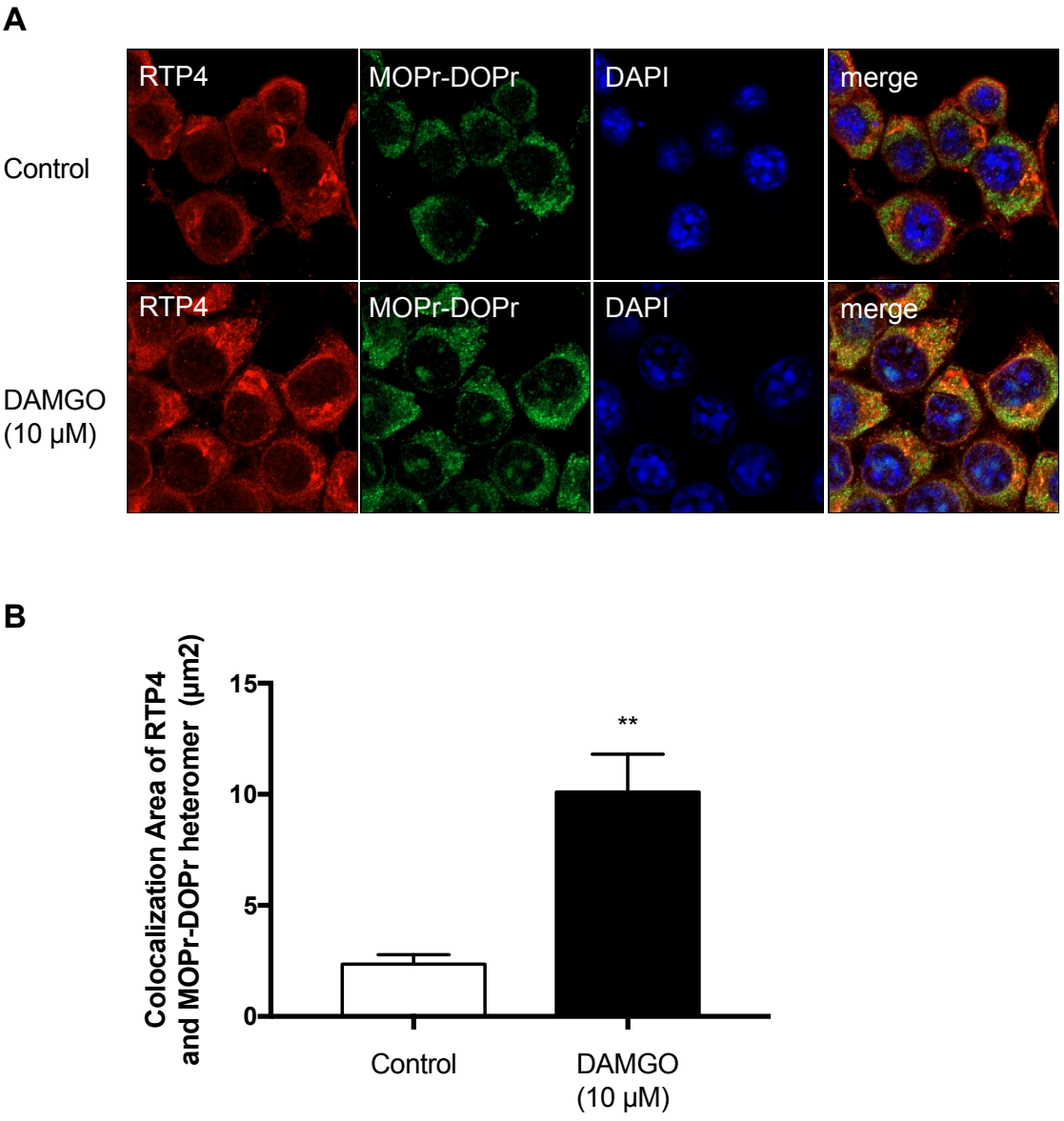
A
RTP4
MOPr-DOPr
DAPI
merge
Control
RTP4
MOPr-DOPr
DAPI
merge
DAMGO
(10 μM)
B
Colocalization Area of RTP4
and MOPr-DOPr heteromer (μm2)
15
10
5
0
**
Control
DAMGO
(10 μM)